Nanoscale Research Letters
a SpringerOpen Journal

NANO EXPRESS Open Access

Improved characteristics of near-band-edge and deep-level emissions from ZnO nanorod arrays by atomic-layer-deposited Al_2O_3 and ZnO shell layers

Wen-Cheng Sun[1,2], Yu-Cheng Yeh[1,2], Chung-Ting Ko[1], Jr-Hau He[2*] and Miin-Jang Chen[1*]

Abstract

We report on the characteristics of near-band-edge (NBE) emission and deep-level band from ZnO/Al_2O_3 and ZnO/ZnO core-shell nanorod arrays (NRAs). Vertically aligned ZnO NRAs were synthesized by an aqueous chemical method, and the Al_2O_3 and ZnO shell layers were prepared by the highly conformal atomic layer deposition technique. Photoluminescence measurements revealed that the deep-level band was suppressed and the NBE emission was significantly enhanced after the deposition of Al_2O_3 and ZnO shells, which are attributed to the decrease in oxygen interstitials at the surface and the reduction in surface band bending of ZnO core, respectively. The shift of deep-level emissions from the ZnO/ZnO core-shell NRAs was observed for the first time. Owing to the presence of the ZnO shell layer, the yellow band associated with the oxygen interstitials inside the ZnO core would be prevailed over by the green luminescence, which originates from the recombination of the electrons in the conduction band with the holes trapped by the oxygen vacancies in the ZnO shell.
PACS 68.65.Ac; 71.35.-y; 78.45.+h; 78.55.-m; 78.55.Et; 78.67.Hc; 81.16.Be; 85.60.Jb.

Introduction

Because of large surface-to-volume ratio and spatial confinement of carriers, researches on one-dimensional (1D) nanostructures have attracted great interest [1-3], and remarkable progress has been achieved in various electronic, photonic, and sensing devices [3-7]. Novel synthetic approaches to the fabrication of high-quality semiconductor nanotubes have been reviewed by Yan et al. [8]. Zinc oxide (ZnO) has been regarded as one of the most promising materials for 1D nanostructures due to its distinguished characteristics such as direct and wide band gap (approximately 3.37 eV), large excitonic binding energy (up to 60 meV), and high piezoelectricity [9-11]. The synthesis of well-aligned ZnO nanorod arrays (NRAs) is crucially important for the practical applications such as field emitters [12], nanogenerators [13], solar cells [14], and nanolasers [15]. One of the popular techniques for fabricating ZnO NRAs is to use Au as catalyst on a lattice-matched substrate [16]. Since the optical properties of ZnO NRAs are strongly dependent on surface conditions [17-20] and natural defect states [21-24], a large variety of surface modifications on ZnO NRAs have been carried out by depositing a shell layer. For instance, the enhancement of photoluminescence (PL) has been observed in ZnO/Er_2O_3 and ZnO/MgZnO core-shell NRAs [25,26]. The enhanced surface-excitonic emission together with the suppression in deep-level emission has also been reported in ZnO/amorphous-Al_2O_3 core-shell nanowires [27]. Apart from the enhancement of light emission, strong photoconductivity [28], photocatalytic activity [29], and quantum confinement [30] have been observed in various 1D ZnO nanostructures.

In this paper, vertically aligned ZnO NRAs were synthesized using an aqueous chemical method, which is beneficial for low reaction temperature, low cost, catalyst-free synthesis, and large-scale production. The growth of ZnO NRAs was assisted by a ZnO seed layer prepared by atomic layer deposition (ALD). The self-limiting and layer-by-layer growth of ALD contribute to many advantages such as easy and accurate thickness control, conformal step coverage, high uniformity over a large area, low defect density, good reproducibility, and low deposition

* Correspondence: jhhe@cc.ee.ntu.edu.tw; mjchen@ntu.edu.tw
[1]Department of Materials Science and Engineering, National Taiwan University, Taipei 10617, Taiwan
[2]Graduate Institute of Photonics and Optoelectronics, National Taiwan University, Taipei 10617, Taiwan
Full list of author information is available at the end of the article

temperature. Therefore, highly conformal Al_2O_3 and ZnO shell layers could be deposited upon the surface of ZnO nanorods by ALD to form the ZnO/Al_2O_3 and ZnO/ZnO core-shell NRAs in this study. PL measurements were conducted to investigate the optical characteristics of ZnO/Al_2O_3 and ZnO/ZnO core-shell NRAs. The near-band-edge (NBE) emission was significantly enhanced, and the deep-level band was suppressed by the Al_2O_3 and ZnO shells due to the flat-band effect and the reduction in the surface defect density. In addition, the shift of deep-level emissions from the yellow band to the green band in ZnO/ZnO core-shell structure was reported. The mechanisms of flat-band effect and the shift of deep-level emissions were elucidated in detail.

Experimental details

The ZnO NRAs were synthesized on (100) Si wafers by aqueous chemical growth. Before the synthesis, a 50-nm-thick ZnO seed layer was deposited on the wafer at a temperature of 180°C by ALD. Diethylzinc and H_2O vapors were used as the precursors for zinc and oxygen, respectively. After the ALD deposition, the seed layer was treated by rapid thermal annealing at 950°C for 5 min in nitrogen atmosphere to improve its crystal quality. Afterwards, the ZnO NRAs were grown in 320 ml aqueous solution, containing 10 mM zinc nitrate hexahydrate and 5 ml ammonia solution, at 95°C for 2 h. More details of ZnO NRA synthesis have been described elsewhere [31,32]. Finally, Al_2O_3 and ZnO shell layers were prepared by the ALD on the as-grown ZnO NRAs to fabricate ZnO/Al_2O_3 and ZnO/ZnO core-shell NRAs. The precursors for Al_2O_3 deposition were trimethylaluminum and H_2O vapors, and the deposition temperature was 180°C. The Al_2O_3 shell layers were 2, 5, and 10 nm in thickness. The ALD condition of ZnO shell layers was the same as that of the ZnO seed layer. The thicknesses of ZnO shell layers were 5, 10, and 15 nm, respectively. The details of ZnO and Al_2O_3 ALD parameters can be found in our previous studies [33-35].

The structural characterization of ZnO NRAs was examined by Germini LEO 1530 field emission scanning electron microscopy (SEM) (**Carl Zeiss Microscopy**, Carl-Zeiss-Straße 56, 73447 Oberkochen, Germany) and FEI Tecnai G2 T20 transmission electron microscopy (TEM) (**FEI Company**, 5350 NE Dawson Creek Drive, Hillsboro, Oregon 97124 USA). X-ray diffraction (XRD) measurement was used to characterize the crystallinity and crystal orientation of ZnO NRAs. PL spectroscopy was measured in a standard backscattering configuration where the light emission from top surface of the ZnO NRAs was collected, using a continuous-wave He-Cd laser (λ = 325 nm) as the excitation source.

Results and discussion

Top-viewed and cross-sectional SEM images of as-grown ZnO NRAs are shown in Figure 1a,b, respectively. The diameter of ZnO nanorods is in the range of 90 to 100 nm, and the length is about 1 μm. The substrate-bound NRAs were mechanically scraped, sonicated in ethanol, and deposited on carbon-coated copper grids for TEM characterization. Figure 1c,d shows low-magnification TEM images of ZnO/Al_2O_3 and ZnO/ZnO core-shell nanorods, indicating the uniformity in both of the core and shell layers. It can be seen that about 5 nm Al_2O_3 and 10 nm ZnO shell layers were deposited upon the surface of ZnO nanorods, demonstrating high conformality of the ALD technique. XRD pattern of as-grown ZnO NRAs is shown in Figure 1e, and the only dominant peak corresponding to (0002) plane was observed in the spectrum, revealing that ZnO nanorods are highly *c*-axis orientated. Moreover, it was noted that ZnO NRAs cannot be synthesized on (100) Si wafers without the ZnO seed layer.

Figure 2a shows the room-temperature PL spectra of as-grown ZnO NRAs and those coated with the Al_2O_3 shell layers. Both the NBE emission ($\lambda \approx$ 380 nm) and deep-level band associated with the oxygen interstitials (O_i) ($\lambda \approx$ 550 nm, yellow band) [22] were observed in the as-grown ZnO NRAs and ZnO/Al_2O_3 core-shell NRAs. As compared with as-grown ZnO NRAs, the NBE emission was significantly enhanced and the deep-level band was suppressed for the samples coated with Al_2O_3 shell layers. The intensity of NBE emission grows along with the increase of the Al_2O_3 shell-layer thickness. The deep-level band also increases slightly with the thickness of the Al_2O_3 shell layer. The PL spectra normalized to the peak intensity of each NBE emission are shown in Figure 2b. It can be seen that the ratio of the deep-level band to the NBE emission of the samples coated with Al_2O_3 shell layers is much smaller than that of as-grown ZnO NRAs. It may be also noted that the ratio of deep-level band to the NBE emission is almost identical for the ZnO/Al_2O_3 core-shell NRAs with different shell-layer thickness, suggesting that the same mechanism governs the increase of the NBE and deep-level emissions with the Al_2O_3 shell-layer thickness.

As compared with the deep-level band of as-grown ZnO NRAs, the considerable suppression of the deep-level luminescence by the deposition of Al_2O_3 shell layers, as shown in Figure 2a,b, can be ascribed to the decrease in the density of oxygen interstitials at the surface of ZnO core [36]. The residual deep-level emission from the ZnO/Al_2O_3 core-shell NRAs may mainly originate from the oxygen interstitials inside the ZnO core. On the other hand, the remarkable enhancement of the ZnO NBE emission by depositing Al_2O_3 shell layers can

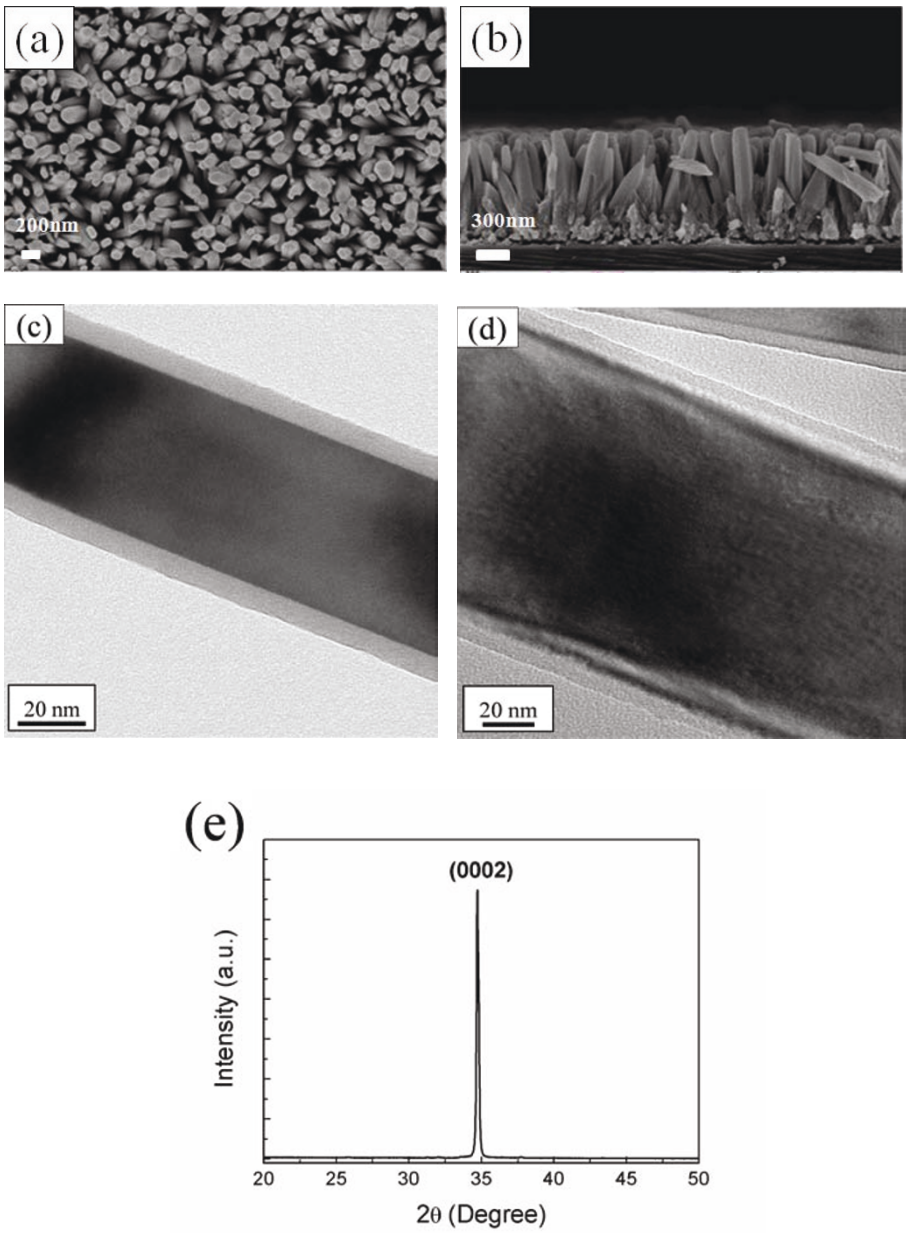

Figure 1 SEM images, TEM images, and XRD pattern. (**a**) Top-viewed and (**b**) cross-sectional SEM images of as-grown ZnO NRAs, (**c**) TEM image of the ZnO core with approximately 5 nm Al_2O_3 shell, (**d**) TEM image of the ZnO core with approximately 10 nm ZnO shell, and (**e**) XRD pattern of as-grown ZnO NRAs.

be attributed to the flat-band effect [27,37]. Negatively charged oxygen ions may adsorb on the surface of as-grown ZnO nanorods, resulting in a depletion region near the surface [38]. Weber et al. have reported that the width of depletion region is about 20 nm [39], which is smaller than the diameter of the ZnO nanorods (approximately 100 nm) prepared in this study. This depletion region can be regarded as an upward band bending toward the surface as presented in the band diagram shown in Figure 3a. When the ZnO NRAs are irradiated by the pumping laser beam, the photo-generated holes are inclined to accumulate near the surface, and the photo-generated electrons tend to reside inside the core. As a result, the wavefunctions of electrons and holes are separated from each other, lowering the probability of radiative recombination to yield NBE emission. However, as plotted schematically in Figure 3b, the Al_2O_3 shell layer would eliminate the oxygen ions adsorbed on the ZnO surface and hence reduce the band bending near the interface [27]. Therefore, the

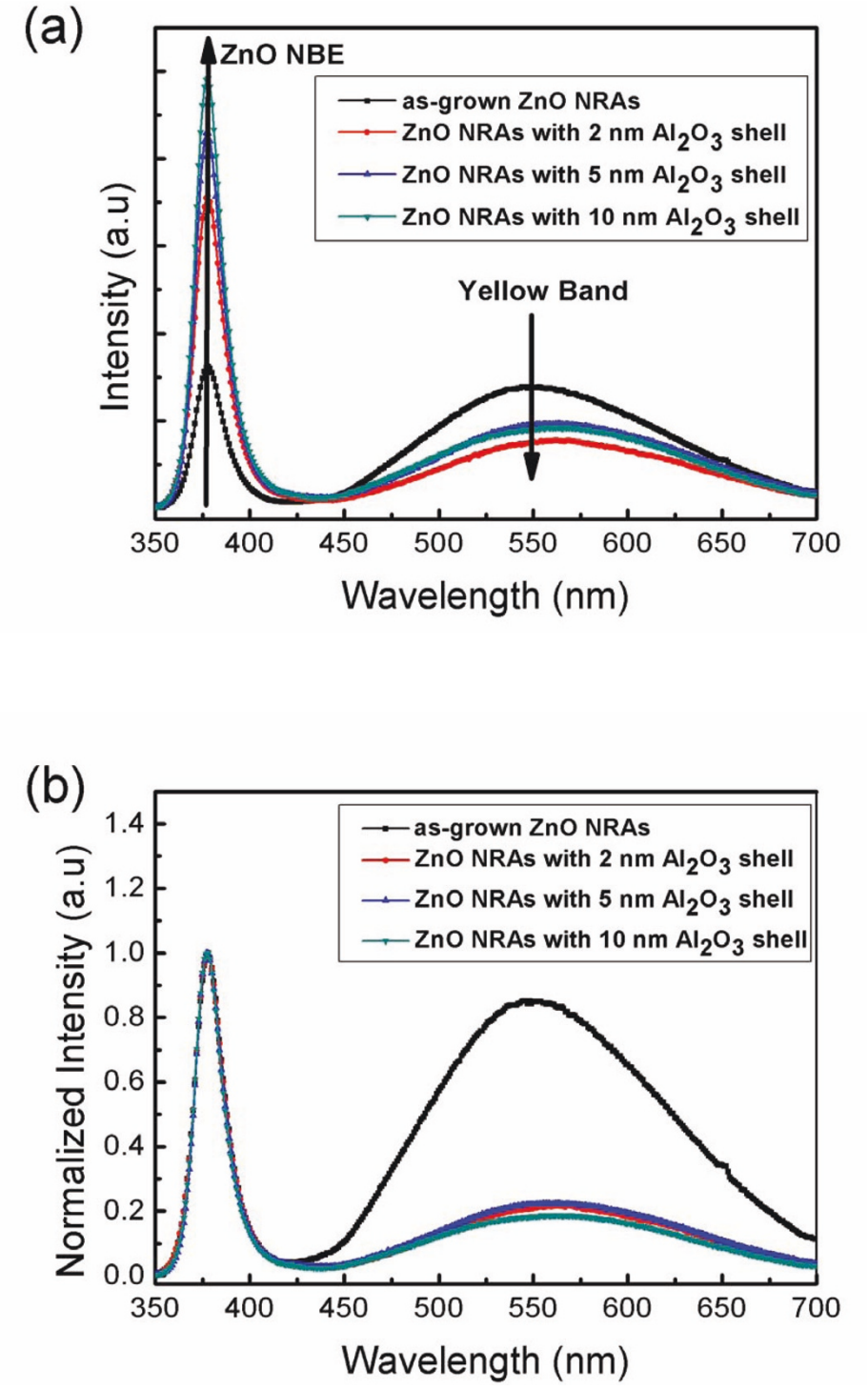

Figure 2 PL spectra. (**a**) Room-temperature PL spectra of as-grown ZnO NRAs and those coated with Al_2O_3 shell layers of different thicknesses. (**b**) Normalized PL spectra of (a). The PL spectra were normalized to the peak intensity of the NBE emission.

overlap between the wavefunctions of electrons and holes in the ZnO core is increased, leading to the enhancement of NBE emission. The increase of the Al_2O_3 shell-layer thickness from 2 to 10 nm may further lower the band bending near the interface and thus enhance the wavefunction overlap, resulting in the increase in NBE emission with the thickness of the Al_2O_3 shell layer. The same argument also holds for

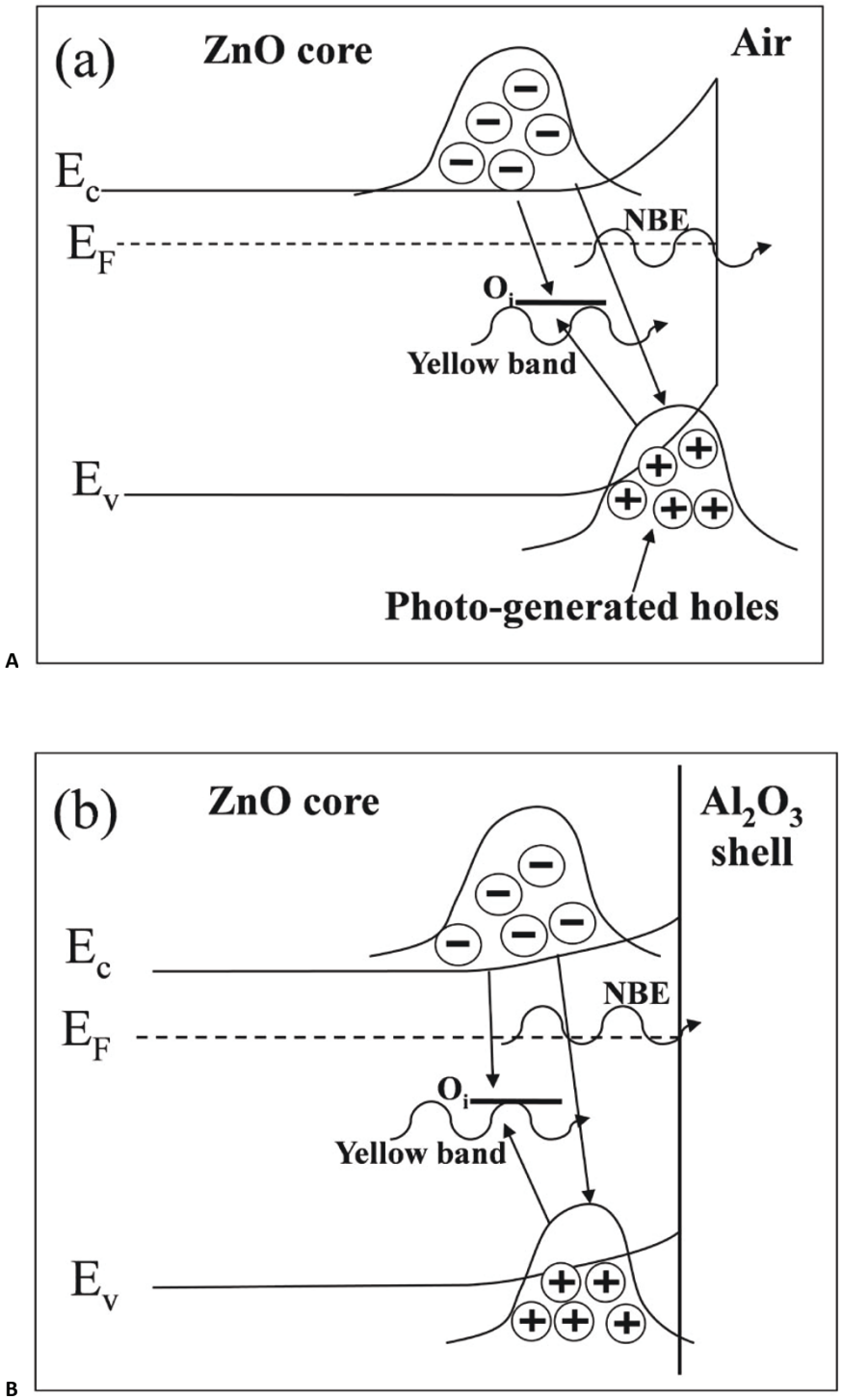

Figure 3 Band diagrams. Schematic band diagrams of (a) as-grown ZnO NRAs and (b) ZnO/Al_2O_3 core-shell NRAs.

the carrier recombination through the deep-level states inside the ZnO core. As illustrated in Figure 3a,b, the flat-band effect may also enhance the deep-level emission around $\lambda \approx 550$ nm originating from the oxygen interstitials inside the ZnO core due to the increase of the wavefunction overlap. Accordingly, as shown in Figure 2b, the normalized PL spectra present almost the same ratio of the deep-level band to the NBE emission

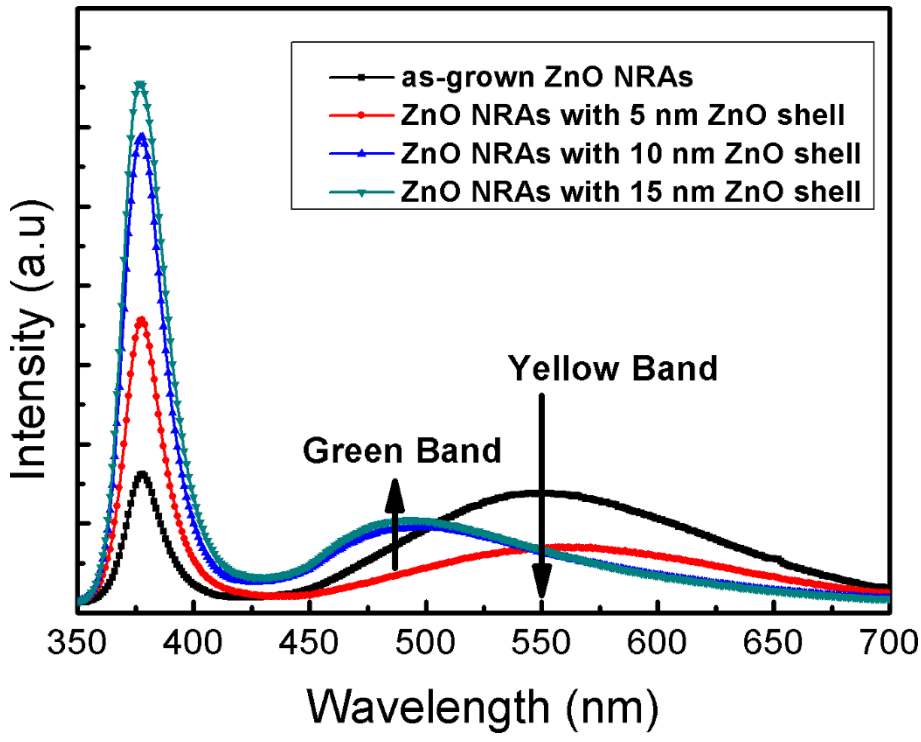

Figure 4 PL spectra. Room-temperature PL spectra of as-grown ZnO NRAs and those coated with ZnO shell layers of different thicknesses.

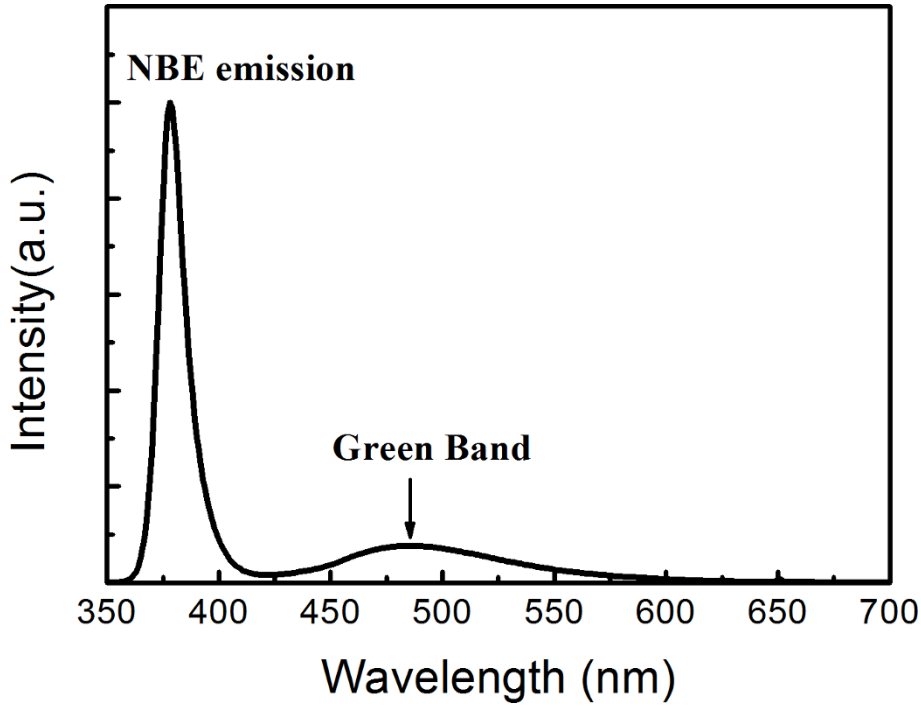

Figure 5 PL spectrum. Room-temperature PL spectrum of the ZnO seed layer grown by ALD.

for the NRAs with different Al_2O_3 shell-layer thickness, indicating that the increase of the Al_2O_3 shell-layer thickness enhances both the NBE and deep-level emissions due to the flat-band effect.

To further investigate the effect of surface band bending in ZnO nanorods, we conducted the PL measurement on ZnO/ZnO core-shell NRAs with different thicknesses of ZnO shell layers. Since the absorption coefficient of

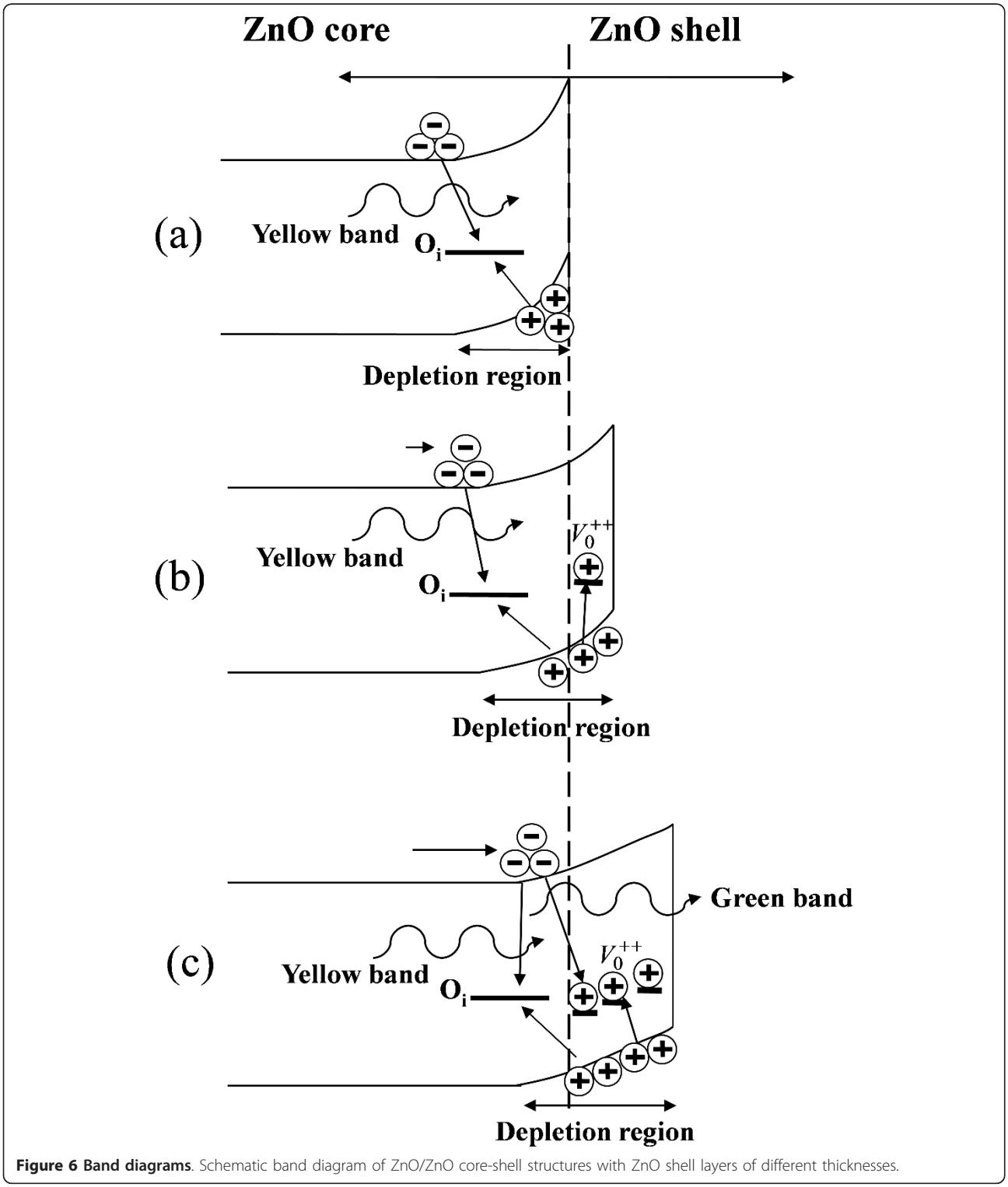

Figure 6 Band diagrams. Schematic band diagram of ZnO/ZnO core-shell structures with ZnO shell layers of different thicknesses.

ZnO at λ = 325 nm is about 1.5 × 10^5 cm^{-1} [40] and the estimated penetration depth is approximately 67 nm, both ZnO cores and ZnO shells could be excited by the He-Cd laser during the PL measurement. Figure 4 shows the PL spectra of the as-grown ZnO NRAs and ZnO/ZnO core-shell NRAs at room temperature. As compared with as-grown ZnO NRAs, the NBE emission was enhanced and the deep-level band around 550 nm was suppressed after a 5-nm-thick ZnO shell layer was deposited. This can be realized that the ZnO shell layer could give rise to the increase of the flat-band region in the ZnO core and the reduction in the density of oxygen interstitials at the surface of ZnO core. Similar to the ZnO/Al_2O_3 core-shell NRAs, the residual deep-level band around $\lambda \approx$ 550 nm of the NRAs coated with a 5-nm-thick ZnO shell layer can be attributed to light emission from the oxygen interstitials inside the ZnO core.

Figure 4 also presents the remarkable shift of the defect-related luminescence, from the yellow band (approximately 550 nm) to the green band (approximately 490 nm), as the thickness of the ZnO shell layer is greater than 10 nm. This green band can be also found in the PL spectrum of the ZnO seed layer grown by ALD, as shown in Figure 5, suggesting that the green band may originate from the ALD ZnO shell layer. It has been reported that the green band arises from the recombination of the electrons in the conduction band and the holes trapped by the V_0^+ center (one electron at the site of oxygen vacancy) [27,41]. As shown schematically in Figure 6a, the photo-generated holes are accumulated near the surface of ZnO nanorods due to the surface band bending. As a 5-nm-thick ZnO shell layer was deposited by ALD, the V_0^+ centers in the ZnO shell layer trap the photo-generated holes and then convert to V_0^{++}, as illustrated in Figure 6b. However, the band bending depletes the electrons near the surface so as to suppress the recombination of the electrons and the V_0^{++} centers. As a result, the green band associated with V_0^{++} did not appear; instead, the yellow band from the oxygen interstitials inside the ZnO core was observed in the PL spectrum. Figure 6c shows that the extension of flat-band region in the ZnO core can reach the ZnO/ZnO core-shell interface as the ZnO shell layer is thick enough. Therefore, the V_0^{++} centers can recombine with the electrons in the conduction band to yield the green luminescence. As a result, the green band dominates over the yellow band as the ZnO shell-layer thickness is greater than 10 nm, as shown in the PL spectra in Figure 4.

Conclusion

In summary, the ZnO/Al_2O_3 and ZnO/ZnO core-shell NRAs have been prepared using the aqueous chemical synthesis and the conformal ALD technique. The deep-level emission around $\lambda \approx$ 550 nm from the oxygen interstitials at the surface of ZnO cores was suppressed by the Al_2O_3 and ZnO shell layers. The shell layers also reduce the surface band bending, leading to the increase in overlap of the wavefunctions of electrons and holes in the ZnO core. Therefore, the NBE emission at $\lambda \approx$ 380 nm and the deep-level band around $\lambda \approx$ 550 nm from the oxygen interstitials inside the core were enhanced by the shell layers. Furthermore, the shift of defect-related emissions from the ZnO/ZnO core-shell NRAs was observed due to the competition between light emissions from the oxygen interstitials inside the ZnO core and the oxygen vacancies in the ZnO shell. As the thickness of the ZnO shell layer increased, the green luminescence ($\lambda \approx$ 490 nm) originating from the oxygen vacancies in the shell dominated over the yellow band ($\lambda \approx$ 550 nm) associated with the oxygen interstitials inside the ZnO core due to the flat-band effect. The results indicate that the shell layers prepared by ALD have significant influence both on the NBE and defect-related emissions of the ZnO NRAs.

Acknowledgements

This work was financially supported by the National Science Council in Taiwan under contract number NSC98-2112-M-002-018-MY2 and NSC100-3113-E002-011.

Author details

[1]Department of Materials Science and Engineering, National Taiwan University, Taipei 10617, Taiwan [2]Graduate Institute of Photonics and Optoelectronics, National Taiwan University, Taipei 10617, Taiwan

Authors' contributions

All the authors contributed to the writing of the manuscript. WCS and YCY carried out the experiments under the instruction of MJC. CTK performed the TEM measurement. All authors read and approved the final manuscript.

Competing interests

The authors declare that they have no competing interests.

Received: 2 June 2011 Accepted: 17 October 2011
Published: 17 October 2011

References

1. Sirbuly DJ, Law M, Yan H, Yang P: **Semiconductor nanowires for subwavelength photonics integration.** *J Phys Chem B* 2005, **109**:15190-15213.
2. Fang X, Gautamy UK, Bando Y, Golberg D: **One-dimensional ZnS-based hetero-, core/shell and hierarchical nanostructures.** *J Mater Sci Technol* 2008, **24**:520-528.
3. Appell D: **Nanotechnology: wired for success.** *Nature* 2002, **419**:553-555.
4. Duan XF, Huang Y, Cui Y, Wang JF, Lieber CM: **Indium phosphide nanowires as building blocks for nanoscale electronic and optoelectronic devices.** *Nature* 2001, **409**:66-69.
5. He JH, Ho CH: **The study of electrical characteristics of heterojunction based on ZnO nanowires using ultrahigh-vacuum conducting atomic force microscopy.** *Appl Phys Lett* 2007, **91**:233105.
6. He JH, Hsin CL, Liu J, Chen LJ, Wang ZL: **Piezoelectric gated diode of a single ZnO nanowire.** *Adv Mater* 2007, **19**:781-784.
7. He JH, Lin YH, McConney ME, Tsukruk VV, Wang ZL, Bao G: **Enhancing UV photoconductivity of ZnO nanobelt by polyacrylonitrile functionalization.** *J Appl Phys* 2007, **102**:084303.

8. Yan C, Liu J, Liu F, Wu J, Gao K, Xue D: **Tube formation in nanoscale materials.** *Nanoscale Res Lett* 2008, **3**:473-480.
9. Ozgur U, Alivov YI, Liu C, Teke A, Reshchikov MA, Dogan S, Avrutin V, Cho SJ, Morkocd H: **A comprehensive review of ZnO materials and devices.** *J Appl Phys* 2005, **98**:041301.
10. Jagadish C, Pearton SJ: *Zinc Oxide Bulk, Thin Films and Nanostructures: Processing, Properties and Application* Oxford: Elsevier; 2006.
11. Wu J, Xue D: **Progress of science and technology of ZnO as advanced material.** *Science of Advanced Materials* 2011, **3**:127-149.
12. Huo KF, Hu YM, Fu JJ, Wang XB, Chu PK, Hu Z, Chen Y: **Direct and large-area growth of one-dimensional ZnO nanostructures from and on a brass substrate.** *J Phys Chem C* 2007, **111**:5876-5881.
13. Wang XD, Song JH, Liu J, Wang ZL: **Direct-current nanogenerator driven by ultrasonic waves.** *Science* 2007, **316**:102-105.
14. Law M, Greene LE, Johnson JC, Saykally R, Yang PD: **Nanowire dye-sensitized solar cells.** *Nat Mater* 2005, **4**:455-459.
15. Huang MH, Mao S, Feick H, Yan HQ, Wu YY, Kind H, Weber E, Russo R, Yang PD: **Room-temperature ultraviolet nanowire nanolasers.** *Science* 2001, **292**:1897-1899.
16. He JH, Hsu JH, Wang CW, Lin HN, Chen LJ, Wang ZL: **Pattern and feature designed growth of ZnO nanowire arrays for vertical devices.** *J Phys Chem B* 2006, **110**:50-53.
17. Travnikov VV, Freiberg A, Savikhin SF: **Surface excitons in ZnO crystals.** *J Lumin* 1990, **47**:107-112.
18. Savikhin S, Freiberg A: **Origin of "universal" ultraviolet luminescence from the surfaces of solids at low temperatures.** *J Lumin* 1993, **55**:1-3.
19. Wischmeier L, Voss T, Borner S, Schade W: **Comparison of the optical properties of as-grown ensembles and single ZnO.** *Appl Phys A* 2006, **84**:111-116.
20. Shimpi P, Gao PX, Goberman D, Ding Y: **Low temperature synthesis and characterization of MgO/ZnO composite nanowire arrays.** *Nanotechnology* 2009, **20**:125608.
21. Vanheusden K, Warren WL, Seager CH, Tallant DR, Voigt JA, Gnade BE: **Mechanisms behind green photoluminescence in ZnO phosphor powders.** *J Appl Phys* 1996, **79**:7983-7990.
22. Li D, Leung YH, Djurisic AB, Liu ZT, Xie MH, Shi SL, Xu SJ, Chan WK: **Different origins of visible luminescence in ZnO nanostructures fabricated by the chemical and evaporation methods.** *Appl Phys Lett* 2004, **85**:1601-1603.
23. Hsu NE, Hung WK, Chen YF: **Origin of defect emission identified by polarized luminescence from aligned ZnO nanorods.** *J Appl Phys* 2004, **96**:4671-4673.
24. Kärber E, Raadik T, Dedova T, Krustok J, Mere A, Mikli V, Krunks M: **Photoluminescence of spray pyrolysis deposited ZnO nanorods.** *Nanoscale Res Lett* 2011, **6**:359.
25. Park WI, Yoo J, Kim DW, Yi GC: **Fabrication and photoluminescent properties of heteroepitaxial ZnO/$Zn_{0.8}Mg_{0.2}O$ coaxial nanorod heterostructures.** *J Phys Chem B* 2006, **110**:1516-1519.
26. Li SZ, Gan CL, Cai H, Yuan CL, Guo J, Lee PS, Ma J: **Enhanced photoluminescence of ZnO/Er_2O_3 core-shell structure nanorods synthesized by pulsed laser deposition.** *Appl Phys Lett* 2007, **90**:263106.
27. Richters JP, Voss T, Skim D, Scholz R, Zacharias M: **Enhanced surface-excitonic emission in ZnO/Al_2O_3 core-shell nanowires.** *Nanotechnology* 2008, **19**:305202.
28. Soci C, Zhang A, Xiang B, Dayeh SA, Aplin DPR, Park J, Bao XY, Lo YH, Wang D: **ZnO nanowire UV photodetector with high internal gain.** *Nano Lett* 2007, **7**:1003-1009.
29. Lu HB, Li H, Liao L, Tian Y, Shuai M, Li JC, Hu MF, Fu Q, Zhu BP: **Low-temperature synthesis and photocatalytic properties of ZnO nanotubes by thermal oxidation of Zn nanowires.** *Nanotechnology* 2008, **19**:045605.
30. Yin M, Gu Y, Kuskovsky IL, Andelman T, Zhu Y, Neumark GF, O'Brien S: **Zin oxide quantum rods.** *J Am Chem Soc* 2004, **126**:6206-6207.
31. Yang WC, Wang CW, He JH, Chang YC, Wang JC, Chen LJ, Chen HY, Gwo S: **Facile synthesis of large scale Er-doped ZnO flower-like structures with enhanced 1.54 μm infrared emission.** *Phys Status Solidi A* 2008, **205**:1190-1195.
32. Greene LE, Yuhas BD, Law M, Zitoun D, Yang PD: **Solution-grown zinc oxide nanowires.** *Inorg Chem* 2006, **45**:7535-7543.
33. Chen HC, Chen MJ, Liu TC, Yang JR, Shiojiri M: **Structure and stimulated emission of a high-quality zinc oxide epilayer grown by atomic layer deposition on the sapphire substrate.** *Thin Solid Films* 2010, **519**:536-540.
34. Shih YT, Wu MK, Li WC, Kuan H, Yang JR, Shiojiri M, Chen MJ: **Amplified spontaneous emission from ZnO in *n*-ZnO/ZnO nanodots-SiO_2 composite/*p*-AlGaN heterojunction light-emitting diodes.** *Nanotechnology* 2009, **20**:165201.
35. Chen MJ, Shih YT, Wu MK, Tsai FY: **Enhancement in the efficiency of light emission from silicon by a thin Al_2O_3 surface-passivating layer grown by atomic layer deposition at low temperature.** *J Appl Phys* 2007, **101**:033130.
36. Shalish I, Temkin H, Narayanamurti V: **Size-dependent surface luminescence in ZnO nanowires.** *Phys Rev B* 2004, **69**:245401.
37. Chen CY, Lin CA, Chen MJ, Lin GR, He JH: **ZnO/Al_2O_3 core-shell nanorod arrays: growth, structural characterization, and luminescent properties.** *Nanotechnology* 2009, **20**:185605.
38. Vanheusden K, Seager CH, Warren WL, Tallant DR, Voigt JA: **Correlation between photoluminescence and oxygen vacancies in ZnO phosphors.** *Appl Phys Lett* 1996, **68**:403-405.
39. Weber DH, Beyer A, Völkel B, Gölzhäuser A, Schlenker E, Bakin A, Waag A: **Determination of the specific resistance of individual freestanding ZnO nanowires with the low energy electron point source microscope.** *Appl Phys Lett* 2007, **91**:253126.
40. Muth JF, Kolbas RM, Sharma AK, Oktyabrsky S, Narayan J: **Excitonic structure and absorption coefficient measurements of ZnO single crystal epitaxial films deposited by pulsed laser deposition.** *J Appl Phys* 1999, **85**:7884-7887.
41. Dijken AV, Meulenkamp EA, Vanmaekelbergh D, Meijerink A: **The kinetic of the radiative and nonradiative processes in nanocrystalline ZnO particles upon photoexcitation.** *J Phys Chem B* 2000, **104**:1715-1723.

doi:10.1186/1556-276X-6-556
Cite this article as: Sun *et al.*: Improved characteristics of near-band-edge and deep-level emissions from ZnO nanorod arrays by atomic-layer-deposited Al_2O_3 and ZnO shell layers. *Nanoscale Research Letters* 2011 **6**:556.